

## Transport and magnetic properties of the diluted magnetic semiconductors $\text{Sb}_{1.98-x}\text{V}_{0.02}\text{Cr}_x\text{Te}_3$ and $\text{Sb}_{1.984-y}\text{V}_{0.016}\text{Mn}_y\text{Te}_3$

Č. Drašar<sup>\*1</sup>, J. Kašparová<sup>1</sup>, P. Lošťák<sup>1</sup>, X. Shi<sup>2</sup>, and C. Uher<sup>2</sup>

<sup>1</sup> Faculty of Chemical Technology, University of Pardubice, Čs. Legií Square 565, 532 10 Pardubice, Czech Republic

<sup>2</sup> Department of Physics, University of Michigan, Ann Arbor, MI 48109, USA

Received 20 September 2006, revised 18 December 2006, accepted 3 January 2007

Published online 28 February 2007

PACS 71.20.Nr, 72.15.Gd, 75.50.Pp

We report on electrical transport and magnetic properties of quaternary single crystals of  $\text{Sb}_{1.98-x}\text{V}_{0.02}\text{Cr}_x\text{Te}_3$  and  $\text{Sb}_{1.984-y}\text{V}_{0.016}\text{Mn}_y\text{Te}_3$  with  $x$  ranging from 0 to 0.022 and  $y$  ranging from 0 to 0.034 over temperatures from 2 K to 300 K. Ternary crystals  $\text{Sb}_{2-z}\text{V}_z\text{Te}_3$  were reported to have rather small magnetization in the ferromagnetic state due to low spin of vanadium ions. Therefore, we attempted to combine vanadium with other high-spin elements hoping to enhance both magnetization and the Curie temperature of these diluted magnetic semiconductors (DMS) based on the  $\text{Sb}_2\text{Te}_3$  matrix. While the Curie temperatures of  $\text{Sb}_{1.98-x}\text{V}_{0.02}\text{Cr}_x\text{Te}_3$  samples are comparable to that of  $\text{Sb}_{1.98}\text{V}_{0.02}\text{Te}_3$ , we observe a significant enhancement in the remanent magnetization when Cr is co-doped. In contrast, adding Mn to  $\text{Sb}_{1.984}\text{V}_{0.016}\text{Te}_3$  leads to a decrease in the Curie temperature and, at higher concentrations, to a complete suppression of ferromagnetism. Since Mn enhances the concentration of holes, its presence might seem favorable to the formation of the ferromagnetic order. In reality, the destruction of ferromagnetism in samples containing Mn is likely a result of the antiferromagnetically coupled Mn-ion pairs.

© 2007 WILEY-VCH Verlag GmbH & Co. KGaA, Weinheim

### 1 Introduction

There is an intense research activity concerning the incorporation of magnetic ions into semiconductors. So far, ferromagnetism has been reported in a variety of semiconductor hosts including II–VI [1], III–V [2–4], and group IV [5] tetrahedrally-bonded semiconductors where Mn is the magnetic ion of choice. An informative overview on DMSs and their use in spintronics is given in [6]. Recently, it was found that single crystal forms of  $\text{Sb}_{2-x}\text{V}_x\text{Te}_3$  [7],  $\text{Bi}_{2-x}\text{Fe}_x\text{Te}_3$  [8], and  $\text{Sb}_{2-x}\text{Cr}_x\text{Te}_3$  [9] display ferromagnetic transitions near 23, 12, and 20 K, respectively. Interestingly,  $\text{Sb}_{2-x}\text{Mn}_x\text{Te}_3$  remains paramagnetic down to 2 K [10]. This latter result is in discord with [11] where a claim is made that  $\text{Sb}_{2-x}\text{Mn}_x\text{Te}_3$  is ferromagnetic at low temperatures. However, the experimental evidence presented in [11] merely describes a paramagnetic state. There is no hint of the anomalous Hall effect nor any indication of hysteresis, the two crucial effects necessary to demonstrate the existence of the ferromagnetic state. Low Curie temperatures in single crystals of the transition-metal-doped  $\text{Sb}_2\text{Te}_3$  and  $\text{Bi}_2\text{Te}_3$  are due to low concentrations of active magnetic ions that can be incorporated in the bulk matrix of  $\text{Sb}_2\text{Te}_3$  and  $\text{Bi}_2\text{Te}_3$ . This group of materials has highly anisotropic structure (tetradymite structure) with octahedral coordination, which makes these materials different from all other DMSs. For application of DMSs, both the ferromagnetic transition

\* Corresponding author; e-mail: cestmir.drasar@upce.cz

temperature and the remanent magnetization are important, the latter to increase the spin polarization of band carriers at a given temperature. Ternary crystals of  $\text{Sb}_{2-x}\text{V}_x\text{Te}_3$  display a relatively small magnetization in the ferromagnetic state due to two crucial constraints: low spin of vanadium ions and a rather low solubility of vanadium. On the other hand, they display coercive fields as large as 1.2 T at 2 K and the Curie temperature  $\theta_{\text{CW}} = 23$  K, values comparatively higher than what can be achieved with other magnetic ions in the  $\text{Sb}_2\text{Te}_3$  lattice. Therefore, we attempted to combine vanadium with other “high-spin” ions in order to examine the possibility of cooperative enhancement of the Curie temperature, remanent magnetization, and the coercive field of DMSs based on  $\text{Sb}_2\text{Te}_3$  through enhancements of the overall magnetic ion concentration and the average spin per ion. Although the study is carried out on the highly anisotropic and octahedrally coordinated matrix of  $\text{Sb}_2\text{Te}_3$ , it might provide a guide relevant to other more usual DMSs. The idea of enhancing the magnetic order by a cooperative action of two different magnetic ions could be an attractive approach.

## 2 Experiment

Quaternary single crystals of  $\text{Sb}_{1.98-x}\text{V}_{0.02}\text{Cr}_x\text{Te}_3$  and  $\text{Sb}_{1.984-y}\text{V}_{0.016}\text{Mn}_y\text{Te}_3$  with  $x$  ranging from 0 to 0.022 and  $y$  ranging from 0 to 0.034 were grown using the Bridgman method. The starting polycrystalline materials for growing the single crystals were prepared from 99.999% pure elemental Sb and Te and the doping elements were added in the form of tellurides:  $\text{Cr}_2\text{Te}_3$ ,  $\text{MnTe}_2$  and  $\text{VTe}_2$ . The synthesis of tellurides was carried out by heating stoichiometric mixtures of 5N purity elements to 1300 K for 7 days. The materials were loaded into conical quartz ampoules in the desired stoichiometric ratio and evacuated. The charge was homogenized in a horizontal furnace at a temperature of 1073 K for 48 hours. Single crystals were grown in the same conical ampoules by lowering them through a temperature gradient of 400 K/5 cm at a rate of 1.3 mm/h. This technique yielded single crystals of 5 cm length and 1 cm diameter. Due to directional solidification the concentration of doping elements can vary significantly along the crystal growth direction for a given nominal  $x$  value as was found, for example, previously in the case of Cr [8]. Therefore, specimens for measurements were cut from different locations of single crystals with a spark erosion machine and each of them analyzed individually. Atomic emission spectroscopy (AES) was employed to provide the reported concentrations of chromium, manganese, and vanadium concentrations. From a range of samples we selected those with various contents of Mn and Cr and a fixed content of V. Compositions of the measured samples are given in Table 1. Both transport and magnetic property measurements were carried out on the same samples over the temperature range 2 K to 300 K. Magnetic susceptibility and magnetization measurements were made in a Quantum Design SQUID magnetometer equipped with a 5.5 T magnet. Hall effect and electrical resistivity data were collected in the same instrument with the aid of a Linear Research ac bridge with 16 Hz excitation. The current was perpendicular to the  $c$ -axis for the transport measurements, and the magnetic field was ori-

**Table 1** Compositions and some magnetic and transport properties of measured samples. Parameters of the Curie–Weiss law  $C$ ,  $\chi_0$ ,  $\theta_{\text{CW}}$ , correspond to fits of susceptibility  $\chi = f(T)$  in the temperature interval  $\Delta T = 50\text{--}300$  K. Values of the Hall coefficient  $R_{\text{H}}$  and in-plane resistivity  $\rho$  correspond to  $T = 300$  K.

composition (AES)	$C$ ( $10^{-7}$ K m <sup>3</sup> kg <sup>-1</sup> )	$\chi_0$ ( $10^{-9}$ m <sup>3</sup> kg <sup>-1</sup> )	$\theta_{\text{CW}}$ (K)	$R_{\text{H}}$ (cm <sup>3</sup> C <sup>-1</sup> )	$\rho$ ( $\mu\Omega$ m)
$\text{Sb}_{1.99}\text{V}_{0.010}\text{Te}_3$	0.86	−5	15.6	0.066	4.38
$\text{Sb}_{1.984}\text{V}_{0.016}\text{Te}_3$	2.1	−5.3	21.2	0.067	6.56
$\text{Sb}_{1.974}\text{V}_{0.026}\text{Te}_3$	4.5	−5.9	23.4	0.064	9.81
$\text{Sb}_{1.971}\text{V}_{0.020}\text{Cr}_{0.009}\text{Te}_3$	9.9	−3.5	22.3	0.053	9.82
$\text{Sb}_{1.958}\text{V}_{0.020}\text{Cr}_{0.022}\text{Te}_3$	17.3	−3.4	23.4	0.058	9.25
$\text{Sb}_{1.973}\text{V}_{0.016}\text{Mn}_{0.011}\text{Te}_3$	9.5	−3.6	13.7	0.047	7.71
$\text{Sb}_{1.950}\text{V}_{0.016}\text{Mn}_{0.034}\text{Te}_3$	40	−2.6	−3.1	0.0076	3.02

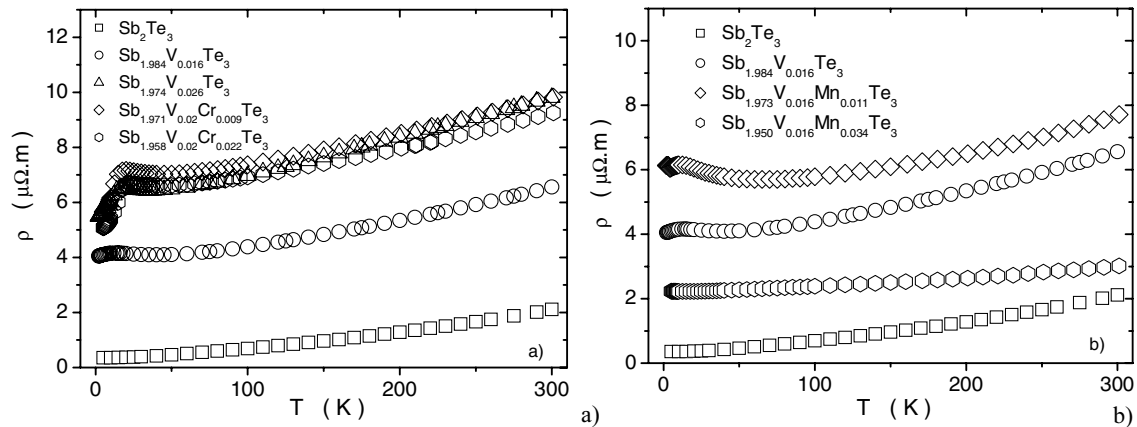


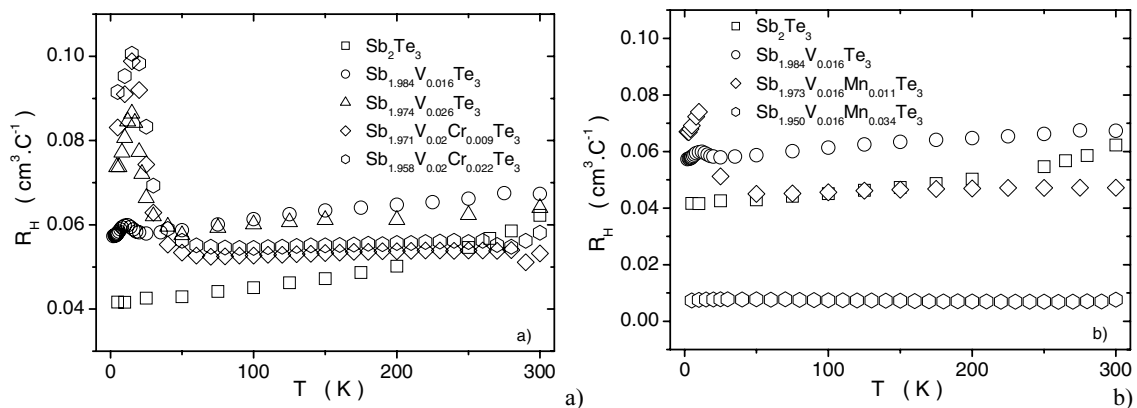
**Fig. 1** Temperature dependence of in-plane resistivity of a)  $\text{Sb}_{1.98-x}\text{V}_{0.02}\text{Cr}_x\text{Te}_3$  and b)  $\text{Sb}_{1.984-y}\text{V}_{0.016}\text{Mn}_y\text{Te}_3$  crystals.

ented parallel to the  $c$ -axis for both the Hall and magnetic measurements. We note that the  $c$ -axis is the easy axis of the magnetization.

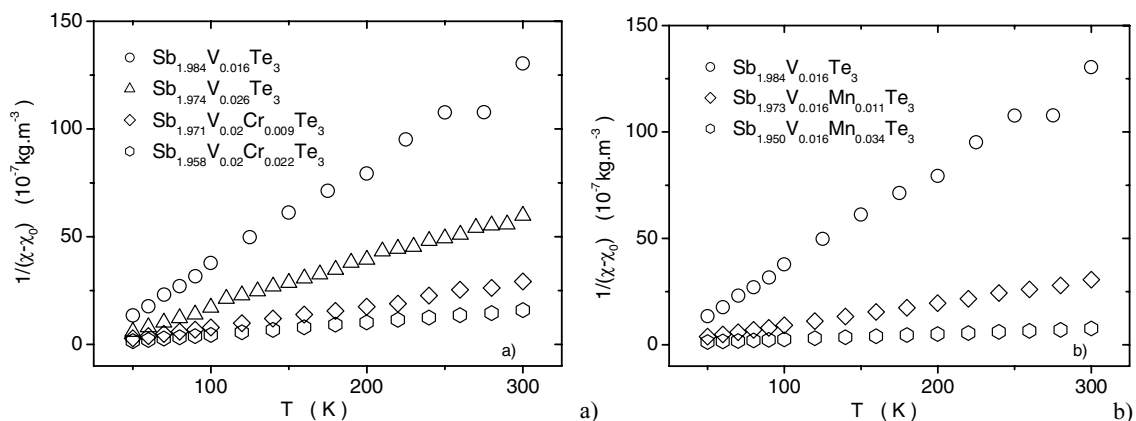
### 3 Results and discussion

Figure 1a and b display the temperature dependence of the in-plane, zero-field electrical resistivity  $\rho$  (current  $\perp c$ -axis) of  $\text{Sb}_{1.98-x}\text{V}_{0.02}\text{Cr}_x\text{Te}_3$  and  $\text{Sb}_{1.984-y}\text{V}_{0.016}\text{Mn}_y\text{Te}_3$ , respectively. The electrical resistivity of pure  $\text{Sb}_2\text{Te}_3$  is dominated by hole conduction and has a dependence characteristic of a degenerate semiconductor ( $p_{\text{Hall}} \approx 10^{20} \text{ cm}^{-3}$  at room temperature). As the concentration of Cr and V in the lattice increases, the electrical resistance increases over the entire temperature range due to an enhancement in point defect scattering. Since Mn acts as an acceptor it increases the concentration of holes in the host  $\text{Sb}_2\text{Te}_3$  matrix and the resistivity tends to decrease [10]. At low temperatures, the resistivity data for all doped samples, except the sample with the highest concentration of Mn, display a maximum suggesting a paramagnetic-ferromagnetic phase transition. Magnetic semiconductors commonly exhibit a maximum in  $\rho$  near their Curie temperature due to enhanced scattering of carriers via exchange interaction with localized spins [12, 13].

Figure 2a and b display the temperature dependence of the Hall coefficient. The results corroborate the measurements of electrical resistivity. While Cr and V have a rather weak influence on the ordinary Hall coefficient, we observe a pronounced decrease of the Hall coefficient with the increasing content of



**Fig. 2** Hall coefficient of a)  $\text{Sb}_{1.98-x}\text{V}_{0.02}\text{Cr}_x\text{Te}_3$  and b)  $\text{Sb}_{1.984-y}\text{V}_{0.016}\text{Mn}_y\text{Te}_3$  as a function of temperature.



**Fig. 3** Inverse magnetic susceptibility  $\chi$  as a function of temperature for a)  $\text{Sb}_{1.98-x}\text{V}_{0.02}\text{Cr}_x\text{Te}_3$ , and b)  $\text{Sb}_{1.984-y}\text{V}_{0.016}\text{Mn}_y\text{Te}_3$  crystals.

manganese due to its acceptor character. Upon analyzing the doping efficiency of Mn in a sample with the highest concentration of Mn atoms ( $\text{Sb}_{1.950}\text{V}_{0.016}\text{Mn}_{0.034}\text{Te}_3$ ) we observe the concentration of holes to rise more than twice as fast as it should had each manganese atom generated one hole [10]. We rechecked this measurement on a sample cut from a different single crystal of the comparable composition using another measurement facility with the same outcome. One plausible explanation of this remarkable effect is a cooperative interaction of V and Mn with the native defects of  $\text{Sb}_2\text{Te}_3$ , rather like the case presented in [14]. We note however, that none of the interactions observed for either V- or Mn-singly doped  $\text{Sb}_2\text{Te}_3$  crystals [7, 10] leads to such a strong shift of hole concentration. The most remarkable feature on the Hall-coefficient data is a sharp rise in the vicinity of the ordering temperature, which can be understood in terms of the anomalous Hall effect. In this case the Hall resistivity is expressed as

$$\rho_{\text{H}} = R_0 B + R_S \mu_0 M, \quad (1)$$

where  $R_0$  is the ordinary Hall coefficient,  $R_S$  is the anomalous Hall coefficient, and  $M$  is the magnetization of the sample. The maximum in  $R_{\text{H}}$  seen in Fig. 2a and b results from a peak in  $R_S$  that is due to asymmetric scattering of conduction carriers (holes) as the spontaneous magnetization develops. Skew scattering was reported as the dominant mechanism in the case of Cr-doped  $\text{Sb}_2\text{Te}_3$  [9]. We note that the maximum disappears with the increasing content of Mn and this indicates a weakening of the ferromagnetic order.

To verify the presence of the magnetic order, measurements of the magnetic susceptibility and field dependence of magnetization were carried out. Figure 3a and b display the temperature dependence of the magnetic susceptibility of  $\text{Sb}_{1.98-x}\text{V}_{0.02}\text{Cr}_x\text{Te}_3$  and  $\text{Sb}_{1.984-y}\text{V}_{0.016}\text{Mn}_y\text{Te}_3$ , respectively. In the paramagnetic region, the data can be fitted nicely using the Curie–Weiss law

$$\chi = \frac{C}{T - \theta_{\text{CW}}} + \chi_0, \quad (2)$$

where  $C$  is the Curie constant,  $\theta_{\text{CW}}$  is the paramagnetic Curie temperature, and  $\chi_0$  is a temperature independent term which takes account of the diamagnetic contributions of the host lattice (see Table 1). We observe the Curie temperatures of Cr–V doped  $\text{Sb}_2\text{Te}_3$  to be comparable to those of the V-doped samples. However, it should be noted that the fitting parameters of the vanadium doped samples (the first three entries in Table 2) are rather dependent on the temperature interval that is being fitted. As documented in Table 2, the value of  $\theta_{\text{CW}}$  decreases when the fitting procedure is carried out over an expanded range of temperatures (making the cut-off at a lower temperature). This suggests that vanadium may have a tendency to form clusters that have a larger  $\theta_{\text{CW}}$  than the rest of vanadium atoms dispersed uni-

**Table 2** Fitting parameters of the Curie–Weiss analysis calculated for two temperature intervals  $50\text{ K} < T < 300\text{ K}$  and  $40\text{ K} < T < 300\text{ K}$ .

composition (AES)	$C$ ( $10^{-7}\text{ K m}^3\text{ kg}^{-1}$ )	$\chi_0$ ( $10^{-9}\text{ m}^3\text{ kg}^{-1}$ )	$\theta_{\text{CW}}$ (K)
$\text{Sb}_{1.99}\text{V}_{0.010}\text{Te}_3$	0.86/0.99	−5.0/−5.0	15.6/10.2
$\text{Sb}_{1.984}\text{V}_{0.016}\text{Te}_3$	2.1/2.3	−5.3/−5.3	21.2/16.5
$\text{Sb}_{1.974}\text{V}_{0.026}\text{Te}_3$	4.5/4.8	−5.9/−6.1	23.4/19.9
$\text{Sb}_{1.971}\text{V}_{0.020}\text{Cr}_{0.009}\text{Te}_3$	9.9/9.9	−3.5/−3.5	22.3/22.3
$\text{Sb}_{1.958}\text{V}_{0.020}\text{Cr}_{0.022}\text{Te}_3$	17.3/17.2	−3.4/−3.4	23.4/23.5
$\text{Sb}_{1.973}\text{V}_{0.016}\text{Mn}_{0.011}\text{Te}_3$	9.5/9.2	−3.6/−3.4	13.7/14.7
$\text{Sb}_{1.950}\text{V}_{0.016}\text{Mn}_{0.034}\text{Te}_3$	40/39	−2.6/−2.2	−3.1/−1.8

formly in the host matrix. Somewhat surprisingly, this tendency seems to be more pronounced at a lower nominal content of vanadium. We note that samples doped with Cr also displayed a similar behavior [9]. Surprisingly, the tendency to cluster disappears in samples co-doped with both chromium and vanadium.

Electronic states of the magnetic ions in the octahedral tellurium coordination have been widely discussed in our previous papers [7, 9, 10, 14]. While vanadium and chromium approach  $3+$  states when substituting for  $\text{Sb}^{3+}$  and thus have a minor influence on the free carrier concentration, manganese ions attain  $2+$  valence and thus raise the hole concentration roughly by one hole per Mn atom. We note that similar results were reported for  $\text{Sb}_{2-x}\text{Cr}_x\text{Te}_3$  in [15]. The presence of two different magnetic ions makes it however difficult to carry an analysis and discussion of electronic states due to an increase in the number of parameters which have to be fitted. Since we treat diluted systems we suppose that the electronic states of the doping elements are similar in the double doped materials.

Upon introducing Mn into the matrix, we observe that the ferromagnetic state progressively weakens and eventually disappears. We also note that  $\chi_0$  becomes less negative for a sample with the highest content of Mn, a scenario that is consistent with a larger Pauli paramagnetic contribution due to the higher density of holes. A possible explanation for the suppression of ferromagnetism in this case might be an antiferromagnetic coupling between Mn ions (superexchange interaction between Mn-ion pairs or Mn–V pairs via the Te sites) that is known to have a deleterious effect on ferromagnetism in Mn-doped II–IV compounds [16] and perhaps even the influence of an exponential term in the exchange integral  $J_{ij}$  given by

$$J_{i,j} = -\frac{2mk_{\text{F}}^4}{\pi h^2} J_{\text{pd}}^2 F(2k_{\text{F}}r_{ij}) \exp\left(-\frac{r_{ij}}{l_{\text{h}}}\right). \quad (3)$$

**Table 3** Overall concentration of ions  $c_{\text{V+Cr+Mn}}$ , the average distance between the ions  $r_{ij} = (1/c_{\text{V+Cr+Mn}})^{1/3}$ , the Hall concentration  $h_{\text{H}} = 1/eR_{\text{H}}$ , the Hall mobility  $\mu_{\text{H}} = R_{\text{H}}/\rho$ , and the mean-free path of holes  $l_{\text{h}}$  as a function of composition at  $T = 100\text{ K}$ . The values for the mean-free path were computed using the formal Drude analysis.

composition (AES)	$c_{\text{V+Cr+Mn}}$ ( $10^{25}\text{ m}^{-3}$ )	$r_{ij}$ ( $10^{-9}\text{ m}$ )	$h_{\text{H}}$ ( $10^{26}\text{ m}^{-3}$ )	$\mu_{\text{H}}$ ( $\text{m}^2\text{ V}^{-1}\text{ s}^{-1}$ )	$l_{\text{h}}$ ( $10^{-9}\text{ m}$ )
$\text{Sb}_{1.99}\text{V}_{0.010}\text{Te}_3$	2.4	3.4	1.09	0.0151	2.2
$\text{Sb}_{1.984}\text{V}_{0.016}\text{Te}_3$	3.9	3.0	1.02	0.0102	1.3
$\text{Sb}_{1.974}\text{V}_{0.026}\text{Te}_3$	6.3	2.5	1.04	0.0065	0.83
$\text{Sb}_{1.971}\text{V}_{0.020}\text{Cr}_{0.009}\text{Te}_3$	7.1	2.4	1.19	0.0054	0.72
$\text{Sb}_{1.958}\text{V}_{0.020}\text{Cr}_{0.022}\text{Te}_3$	10.0	2.1	1.15	0.0064	0.78
$\text{Sb}_{1.973}\text{V}_{0.016}\text{Mn}_{0.011}\text{Te}_3$	6.6	2.5	1.37	0.0061	0.83
$\text{Sb}_{1.950}\text{V}_{0.016}\text{Mn}_{0.034}\text{Te}_3$	12.2	2.0	8.41	0.0025	0.60

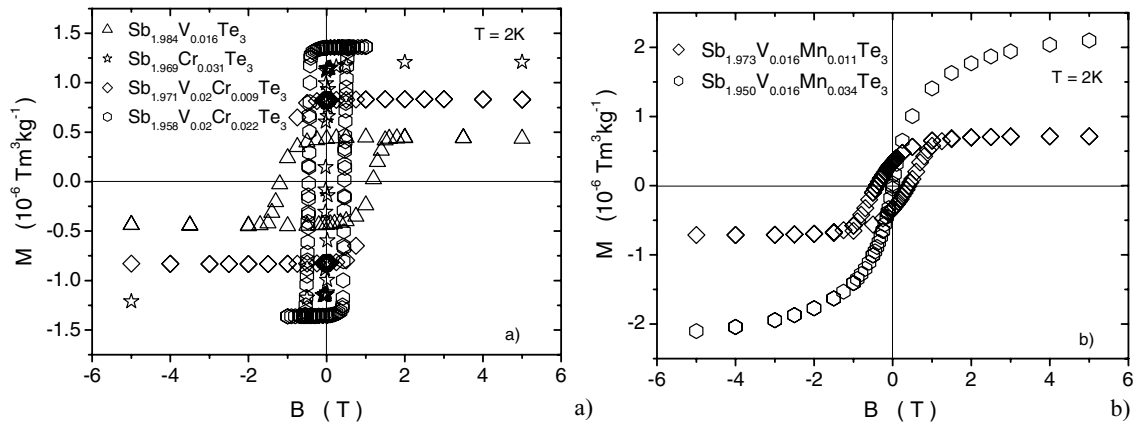


**Fig. 4** Field dependence of magnetization measured at  $T = 2$  K for a)  $\text{Sb}_{1.98-x}\text{V}_{0.02}\text{Cr}_x\text{Te}_3$  and b)  $\text{Sb}_{1.984-y}\text{V}_{0.016}\text{Mn}_y\text{Te}_3$  crystals.

Here  $m$  is the effective mass of carriers,  $k_F$  is the Fermi wave vector,  $h$  is the Planck constant,  $J_{pd}$  the exchange integral between localized spins and free carriers,  $r_{ij}$  is the distance between sites  $i$  and  $j$ ,  $F(2k_F r_{ij})$  is the RKKY oscillation term, and  $l_h$  is the mean free path of holes. Since the mean free path of holes is smaller in the Mn-doped samples, see Table 3, the exponential term in Eq. (3) causes a rapid reduction of the exchange integral.

It should be mentioned that due to the rather complicated band structure and the presence of two types of holes with different masses [17], the transport parameters presented in Table 3 may somewhat differ from the actual parameters. An estimate based on the parameters presented for  $\text{Sb}_2\text{Te}_3$  in paper [17] yields a contribution of heavy holes to  $R_H$  of about 4% due to the fact that the mobility of light holes is by a factor  $\approx 100$  larger than that of heavy holes which are supposed to be the main mediator of interaction among localized spins. We however make a reasonable assumption that the parameters of both types of holes change in the same direction upon doping. Thus, despite the simplification made, the parameters in Table 3 indicate the tendency upon the doping.

We can not rule out other theories. Indeed, regarding the comparable concentrations of holes and of magnetic ions, the Zener mean field theory might be perhaps even more appropriate [18]. Moreover, there is an alternative approach based on spin density functional theory [15] that was applied to Cr-doped  $\text{Sb}_2\text{Te}_3$ . Since we consider double doped systems it would be however rather misleading to figure out the value of  $J_{pd}$  using any of the above theories.

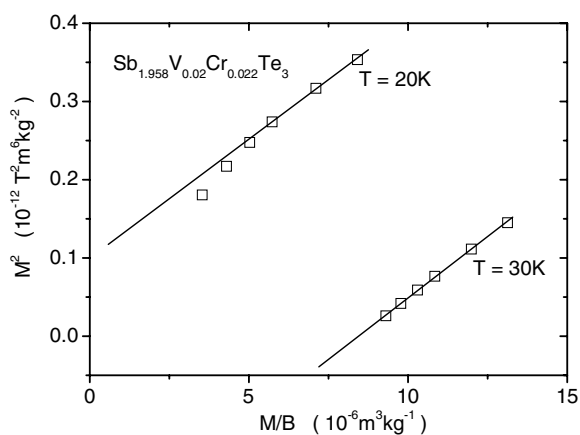


**Fig. 5** Arrott plots for a sample with the highest content of Cr taken at two temperatures around the Curie temperature. The solid lines are high field extrapolations.

Figure 4a and b show the field dependence of the magnetization of  $\text{Sb}_{1.98-x}\text{V}_{0.02}\text{Cr}_x\text{Te}_3$  and  $\text{Sb}_{1.984-y}\text{V}_{0.016}\text{Mn}_y\text{Te}_3$ , respectively. All Cr-doped samples display robust hysteresis loops with the coercive field on the order of 0.5 T and the remanent magnetization that increases with the increasing concentration of Cr ions. For comparison, we show results obtained on single-doped samples of closely matching doping levels. We see that a proper combination of both elements leads to a material with advantageous magnetic properties (a higher remanent magnetization and still a reasonable coercitive field) compared to single doped materials. In contrast, the hysteresis loops become very weak and eventually collapse upon the increasing concentration of Mn. Magnetization measurements thus provide an excellent support for the results of the Curie–Weiss analysis.

In Fig. 5 we include two Arrott plots for  $\text{Sb}_{1.958}\text{V}_{0.02}\text{Cr}_{0.022}\text{Te}_3$  that bracket the actual Curie temperature. It is clear that the ordering temperature of this sample lies above 20 K and the value of  $\theta_{\text{CW}}$  in Table 2 is a reasonable estimate.

## 4 Conclusion

In summary, using the Bridgman technique, we prepared several single crystals in the series  $\text{Sb}_{1.98-x}\text{V}_{0.02}\text{Cr}_x\text{Te}_3$  and  $\text{Sb}_{1.984-y}\text{V}_{0.016}\text{Mn}_y\text{Te}_3$  with the intent to investigate whether double doping with transition metal ions might lead to an enhancement in the Curie temperature of these  $\text{Sb}_2\text{Te}_3$ -based diluted magnetic semiconductors. Although we have not obtained a pronounced improvement in magnetic properties, the double doped crystals show higher remanent magnetization compared to single doped crystals with comparable critical temperature. Our results indicate that the tendency for the magnetic ions to cluster in single doped materials is reduced by double doping. In contrast to co-doping with V and Cr, the presence of Mn in  $\text{Sb}_{2-x}\text{V}_x\text{Te}_3$  leads to a progressive suppression and eventual destruction of the ferromagnetic state. Though the material single-doped with manganese is paramagnetic, Mn ions tend to order antiferromagnetically in double-doped crystals.

**Acknowledgement** This research was supported by the Ministry of Education, Youth and Sports of the Czech Republic under the project MSM 0021627501 and the grant from the National Science Foundation, NSF-DMR-0604549.

## References

- [1] D. Ferrand, J. Cibert, A. Wasiela, C. Bourgonon, S. Tatarenko, G. Fishman, T. Andrearczyk, J. Jaroszynski, S. Kolesnik, T. Dietl, B. Barbara, and D. Dufeu, *Phys. Rev. B* **63**, 085201 (2001).
- [2] H. Munekata, H. Ohno, S. von Molnar, A. Segmüller, L. L. Chang, and L. Esaki, *Phys. Rev. Lett.* **63**, 1849 (1989).
- [3] H. Ohno, A. Shen, F. Matsukura, A. Oiwa, A. Endo, S. Katsumoto, and Y. Iye, *Appl. Phys. Lett.* **69**, 363 (1996).
- [4] T. Wojtowicz, G. Cywinski, W. L. Lim, X. Liu, M. Dobrowolska, J. K. Furdyna, K. M. Yu, W. Walukiewicz, G. B. Kim, M. Cheon, S. M. Wang, and H. Luo, *Appl. Phys. Lett.* **82**, 4310 (2003).
- [5] Y. D. Park, A. T. Hanbicki, S. C. Irwin, C. S. Hellberg, J. M. Sullivan, J. E. Mattson, T. F. Ambrose, A. Wilson, G. Spanos, and B. T. Jonker, *Science* **295**, 651 (2002).
- [6] S. J. Pearton et al., *Mater. Sci. Eng. R* **40**, 137–168 (2003).
- [7] J. S. Dyck, P. Hajek, P. Lostak, and C. Uher, *Phys. Rev. B* **65**, 115212 (2002).
- [8] V. A. Kulbachinskii, A. Yu. Kaminskii, K. Kindo, Y. Narumi, K. Suga, P. Lostak, and P. Svanda, *Physica B* **311**, 292 (2002).
- [9] J. S. Dyck, C. Drašar, P. Lostak, and C. Uher, *Phys. Rev. B* **71**, 115214 (2005).
- [10] J. S. Dyck, P. Svanda, P. Lostak, J. Horak, W. Chen and C. Uher, *J. Appl. Phys.* **94**, 7631 (2003).
- [11] Jeongyong Choi, Sungyool Choi, Jiyoun Choi, Yongsup Park, Hyun-Min Park, Hee-Woong Lee, Byung-Chul Woo, and Sunglae Cho, *phys. stat. sol. (b)* **241**, 1541 (2004).
- [12] F. Matsukura, H. Ohno, A. Shen, and Y. Sugawara, *Phys. Rev. B* **57**, R2037 (1998).
- [13] S. von Molnar and T. Kasuya, *Phys. Rev. Lett.* **21**, 1757 (1968).

- [14] J. Horak, P. Lostak, C. Drasar, J. S. Dyck, Z. Zhou, and C. Uher, *J. Solid State Chem.* **178**, 2907 (2005).
- [15] V. A. Kulbachinskii, P. M. Tarasov, and E. Brück, *Physica B* **386**, 32 (2005).
- [16] T. Dietl, *Semicond. Sci. Technol.* **17**, 377 (2002).
- [17] V. A. Kulbachinskii, Z. M. Dashevskii, M. Inoue, M. Sasaki, H. Negishi, W. Z.-X. Gao, P. Lostak, J. Horak, and A. de Visser, *Phys. Rev. B* **52**, 10915 (1995).
- [18] T. Dietl, H. Ohno, F. Matsukura, J. Cibert, and D. Ferand, *Science* **287**, 5455 (2000).